International Journal of Engineering Technology and Scientific Innovation

ISSN: 2456-1851

Volume: 04, Issue: 05 "September-October 2019"

DESIGN AND OPTIMIZATION OF PERFORMANCE OF A BENCH SCALE GASIFIER FOR SUB-BITUMINOUS COAL

Stellamaris N. Nzove[1*], Hiram Ndiritu[2] and Benson Gathitu[2]

[1,2]Department of Mechanical Engineering, Jomo Kenyatta University of Agriculture and Technology, Kenya, P.O. BOX 62000-00200 Nairobi.

[3]Department of Agricultural and Bio-Systems Engineering, Jomo Kenyatta University Agriculture and Technology, Kenya, P.O. BOX 62000-00200 Nairobi.

[*]Corresponding Author

ABSTRACT

In this research a bench scale gasifier was designed, fabricated and its performance analyzed. The main objective of the research was to develop and optimize the performance of a fluidized bed coal gasifier for production of syngas that can be utilized for power generation. Air flow rate during the gasification process was varied and the reactor temperature and gas composition were measured at each flow rate. Results from this research showed a reduction in carbon monoxide (CO) concentration with increase in airflow rate from 1.0 to 2.5 m^3/min. CO reduction was attributed to fact that more air enhanced conversion of CO to CO_2. As the air flow rate was increased from 1.0 to 2.5 m^3/min, the calorific value of the syngas produced was observed to decrease from 5.667 to 4.106 MJ/Nm^3. This was attributed to the reduction of CO and the increase of nitrogen composition which do not add to the calorific value of the syngas. The optimal equivalence ratio ranged between 0.282 and 0.284. The cold gas efficiency (CGE) and the carbon conversion efficiency of the bench scale gasifier at optimal conditions was 64.29 % and 89.89% respectively.

Keywords: Coal, Fluidized bed, Gasification, Reactor.

1. INTRODUCTION

Over 40% of the world's energy is derived from coal [1]. Coal like other fossil fuels is formed out of carbon and trace amounts of sulphur and nitrogen. When coal burns, carbon dioxide is formed which is a major greenhouse gas and other emissions like NO_x and SO_2 are also formed. NO_x and SO_2 are acidic gases and react with water in the atmosphere forming acidic rain which

ISSN: 2456-1851

Volume: 04, Issue: 05 "September-October 2019"

affects ecosystems. Chang et al. [2] found that 9 billion tonnes of CO_2 were emitted from fuel combustion with more than 83% coming from the combustion of coal. In 2012 about 79% of SO_2, 57% of NO_x and 44% of particulate matter came from direct combustion of coal and about 93% of SO_2 70% of NO_x and 67% of PM emissions came from all kinds of coal utilization (including direct combustion emission and emission from coke stoves and other industrial furnaces).

Coal gasification offers one of the most versatile and clean ways of converting coal into electricity, hydrogen and other valuable energy products. Gasification is a thermo-chemical conversion process by which coal or biomass is partially oxidized to produce a combustible gas or synthetic gas also known as syngas. Syngas comprises of hydrogen (H_2), carbon monoxide (CO), carbon dioxide (CO_2), and methane (CH_4), the proportions being determined by the gasifying agent (air, oxygen, steam or mixture) [3].

Gasification takes place in sub-stoichiometric conditions with controlled oxygen supply generally 20 to 35% of the theoretical oxygen required for complete combustion of coal at temperatures of 700^{o}C and above [4]. The process is such that as coal is consumed, heat and new gaseous fuel is produced [5]. The process of gasification starts with drying since coal contains moisture which can only be removed as steam when the fuel is heated to the saturation temperature of the gasifier operating pressure. What follows is pyrolysis during which light volatile gases such as hydrogen are evolved in addition to other gases, tars and phenols. The resulting char from pyrolysis then reacts with the gaseous reactants (oxygen, steam, carbon dioxide and hydrogen) to release gases (CO, H_2, CO_2, CH_4), tar vapours and a solid residue (char and ash) [6]. Complete gasification is governed by the following set of chemical reactions.

$$C + O_2 \rightarrow CO_2 \qquad 1$$

$$C + \frac{1}{2}O_2 \rightarrow CO \qquad 2$$

$$H_2 + \frac{1}{2}O_2 \rightarrow H_2O \qquad 3$$

$$C + H_2O \rightarrow CO + H_2 \qquad 4$$

$$C + 2H_2O \rightarrow CO_2 + 2H_2 \qquad 5$$

$$C + CO_2 \rightarrow 2CO \qquad 6$$

$$C + 2H_2 \rightarrow CH_4 \qquad 7$$

$$CO + H_2O \rightarrow CO_2 + H_2 \qquad 8$$

$$CO + 3H_2 \rightarrow CH_4 + H_2O \qquad 9$$

$$C + H_2O \rightarrow \frac{1}{2}CH4 + \frac{1}{2}CO_2 \qquad 10$$

Fluidization on the other hand is the process by which fine bed of solids are transformed into a fluid like state through contact with a gas or a liquid. This process promotes proper mixing of the fuel and the oxidizing agent and good heat distribution allowing for uniform temperature within the reactor [7]. Depending on the fluidization velocity the fluidized beds are classified as packed, bubbling or circulating or turbulent [8].

2. EXPERIMENTAL METHODOLOGY

The fluidized bed gasifier consisted of a fluidized bed portion, disengaging space or freeboard (section above the bed of particles) and a gas distributor, solids feeder, solids discharge points, instrumentation and gas supply as shown in Figure 1.

ISSN: 2456-1851

Volume: 04, Issue: 05 "September-October 2019"

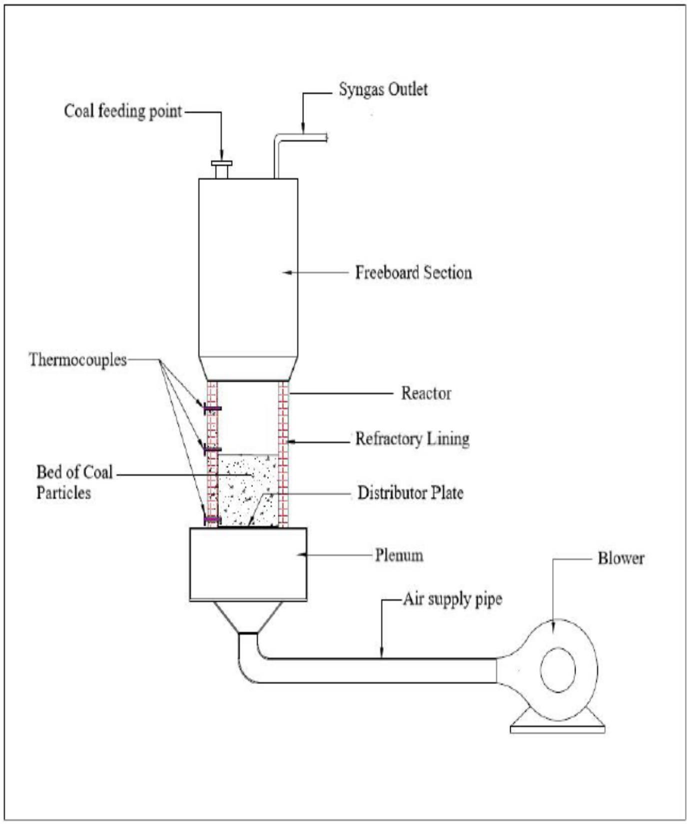

Figure 1: Schematic Diagram of the Bench Scale Gasifier Setup

Design of Bed

Selection of bed height is necessary to ensure sufficiently high residence time of the coal to achieve good carbon conversion in the bed [9]. Excessive heights lead to higher pressure losses and slugging flow within reactor which causes inadequate mass transfer and can lead to mechanical failure of common support structures [10]. Previous studies use the ratio of static height to the bed diameter as 2 for most gasifiers. However, research has shown that if this value is exceeded channeling takes place which is as a result of mesh forming properties of particles [11]. In this research a bed height of 1.5D is adopted where D is the bed diameter. The particle size was chosen to be 3mm according to data compiled by *Basu et al.* [8] which indicated that for fluidized applications the particle size should not exceed 6mm.

From the proximate analysis the density of coal was obtained as 1435 kg/m^3. Most solid particles are irregular in shape and sphericity can be estimated using Expression 11. According to Equation 11 the sphericity of a sphere ϕ_s=1 and for other particles 0≥ ϕ_s ≤1.

ISSN: 2456-1851

Volume: 04, Issue: 05 "September-October 2019"

$$\phi = \frac{S.As}{S.Ap} \qquad 11$$

Where $S.A_s$ and $S.A_p$ are the surface areas of sphere and particle respectively of equal volume. In packed beds, the shape of particles and the particle size distribution influences heat permeability, pressure drop and heat transfer in the reactor [11]. The sphericity of the coal particles in this research was chosen as 0.65 based on criteria by *Kunii, D.* and *Levenspiel* [12].

The void fraction (ε) was estimated using the following model equation developed by *Hartman et al*. [13]. The value was estimated as 0.55.

$$\varepsilon = 1.0 + 0.864\phi_s + 0.2745\phi^2{}_s \qquad 12$$

The frictional pressure drop across the bed was estimated using Ergun equation shown in

$$\frac{\Delta P}{h} = 150\frac{(1-\varepsilon)^2}{\varepsilon^3}\frac{\mu u}{(\phi_s d_p)^2} + 1.75\frac{1-\varepsilon}{\varepsilon^3}\frac{\rho_g u^2}{\phi_s d_p} \qquad 13$$

The pressure drop at the onset of fluidization is equivalent to the weight of the bed so the pressure drop can also be estimated by using the following expression

$$\frac{\Delta P}{h} = W = (\rho_s - \rho_f)(1-\varepsilon)g \qquad 14$$

Where W is the weight of the fluidized particles, ΔP is the pressure drop, ρ_s and ρ_f are densities of coal particles and air respectively.

Minimum fluidization velocity and terminal velocities were estimated using Equation **Error! Reference source not found.** and Equation **Error! Reference source not found.** respectively.

$$u_{mf} = \left(\frac{g(\rho_s - \rho_f)\varepsilon_{mf}^3 d_p}{1.75\rho_f}\right)^{\frac{1}{2}} \qquad 15$$

$$u_t = \frac{g(\rho_s - \rho_f)d_p^2}{18\mu_f} \qquad 16$$

ISSN: 2456-1851

Volume: 04, Issue: 05 "September-October 2019"

The Reactor

The reactor was constructed of a cylindrical tube of diameter 0.315m and length of 0.5m. As the temperatures inside the gasifier can go as high as 1000°C, the inner part of the reactor was lined with refractory clay of thickness 0.03m resulting to an inside diameter of 0.255m. The refractory was used to protect the metal shell from abrasion by bed materials and insulate the shell from elevated temperatures [14]. Two flanges were welded on top and bottom of the reactor to allow for connection to the freeboard section and the support structure respectively. A high temperature gasket seal (Grafoil type) was used between the flanges of the reactor and the support structure to prevent gas leakage. Bolts (M8) and washers were used to join the reactor to the bottom support structure and the upper freeboard section.

The freeboard section was constructed of a mild steel cylindrical tube of diameter 0.38m and a length of 0.5m and a thickness 0.002m. The diameter of the freeboard section is larger than the reactor diameter by 0.065m as recommended by *Ghally et al*. [15]. An increased diameter in the freeboard section is desirable as it allows for reduction of velocity of the produced gas, necessitates return of entrained particles from the bed and also provides more residence time giving complete conversion of tars to lighter hydrocarbon gases [10]. The conversion of high molecular hydrocarbons in tars to light molecular hydrocarbon gases improves the energy content of the syngas [16]. A feeding section was incorporated at the top of the freeboard section to allow for coal feeding. An exit pipe for the syngas was also incorporated as shown in Figure 1.

Distributor plate

The distributor plate plays two main functions which include, supporting the bed material and also has holes or air caps that allow air to flow into the reactor hence initiating effective gas-solids interaction [17]. Proper design of the distributor plate is important to avoid stagnant zones near the grid region which can cause hot spots resulting in agglomeration and eventual failure of the distributor [**18**].

In this research a perforated distributor type was adopted. The distributor was designed based on requirements from *Ghaly et al*.[15], [19]. It was made of a circular steel plate of 315 mm diameter and a thickness of 3mm. A circular area of 220mm diameter was perforated with perforation area being 1.63% of the bed cross-sectional area (255mm). A total of 267 holes of 2mm diameter each were drilled using a triangular pitch of 11.1mm as shown in Figure 2.

ISSN: 2456-1851

Volume: 04, Issue: 05 "September-October 2019"

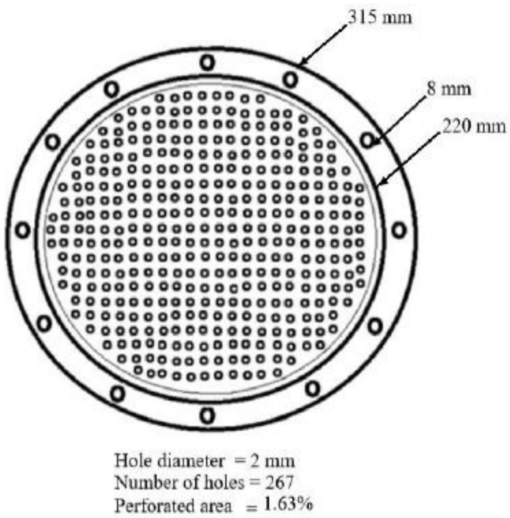

Figure 2: Distributor Plate

Air Supply System

The air supply system consisted of a blower and a piping of 50.8 mm connecting the blower to the plenum section of the support structure. The blower was rated at 600W and with a maximum flow rate of 3.5m^3/min.

Gasifier Performance

The performance of the fluidized bed gasifier was obtained by determining both the cold gas efficiency (CGE) and the carbon conversion efficiency (CCE). CGE refers to the ratio of the energy content of the syngas produced and the energy content of the fuel fed in the gasifier [2**0**]. The energy content of the syngas was obtained by multiplying the net HHV of the syngas and its flow rate, whereas the energy content of the coal was obtained by multiplying the HHV of coal and its consumption rate as shown in

Equation 17. CGE is determined from concentrations of H_2, CO and CH_4.

$$CGE(\%) = \left(\frac{\dot{m}_{out}(y_{H_2} HHV_{H_2} + y_{CO} HHV_{CO} + y_{CH_4} HHV_{CH_4})}{\dot{m}_{inF}\, HHV_F} \right) \qquad 15$$

ISSN: 2456-1851

Volume: 04, Issue: 05 "September-October 2019"

Carbon conversion efficiency is the ratio of fuel carbon which is converted into non-condensable gaseous carbon components to the total fed carbon. CCE is evaluated from concentrations of CO_2, CO and CH_4 as shown Equation 18;

$$CCE(\%) = \left(1 - \frac{\dot{m}_{out}(y_{CO_2}\frac{12}{44} + y_{CO}\frac{12}{28} + y_{CH_4}\frac{12}{16}}{\dot{m}_{inF}\ y_c} \right) \times 100 \qquad 16$$

Where m_{out} is the mass flow rate of the syngas, m_{inF} is the fuel consumption rate, y_i is the mole fraction indices of species i in the product gas and HHV is the higher heating value of the respective constituents of the syngas.

Experimental procedure

Gasification process started by first heating charcoal inside the reactor to 650^{o}C, temperatures at which coal can self-ignite. Coal was then fed from the top of the gasifier and air introduced from the bottom of the reactor at a controlled rate. The operation and monitoring of the gasification process involved controlling the air and coal input, the temperatures inside the reactor were measured using k-type thermocouples and gas composition analyzed using Testo 350-S/-XL gas analyzer. Data from this monitoring was recorded and analyzed.

3. RESULTS AND DISCUSSION

The proximate and ultimate analysis of the coal used in the research are shown in Table 1 and Table 2 respectively.

ISSN: 2456-1851

Volume: 04, Issue: 05 "September-October 2019"

Table 1: Proximate analysis results of coal

Coal Property	Average Value
Bulk Density	1.4347 g/cm^3
Moisture Content	4.09%
Ash Content	13.99%
Calorific Value	30.443MJ/Kg
Fixed Carbon	42.62%

Table 2: Ultimate analysis results of coal

Constituents	% by weight (kg)
Carbon	65.44
Hydrogen	4.6
Oxygen	7.82
Nitrogen	1.07
Sulphur	3.61

The syngas composition and the reactor temperatures are shown in Table 3.

Table 3: Syngas composition and reactor temperature

Air flow rate (m^3/min)	CO	CO_2	H_2	CH_4	Temp (^oC)
1	20.61	15.17	9.6	4.62	850
1.5	22.92	14.61	7.16	3.92	857
2	18.29	15.57	6.94	3.17	861
2.5	17.78	16.23	5.69	2.85	873

ISSN: 2456-1851

Volume: 04, Issue: 05 "September-October 2019"

Effect of air flow rate on product distribution

The composition of the syngas was noted to vary with increase in air flow rate from 1.0 to 2.5m^3/min as shown in Figure 3. The concentration of CO first increased then started to decrease. On the other hand, the concentration of CO_2 decreased first then it started to increases as the air flow rate was increased further. The concentrations of hydrogen decreases with increase in air flow rate.

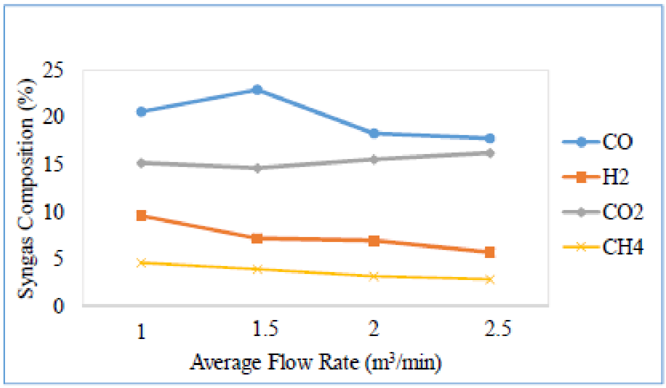

Figure 3: Syngas composition variation with air flow rate

Hydrogen concentrations remained significantly low throughout the tests. Increasing air flow rate increases the amount of oxygen required for exothermic reactions 1, 2 and 3.These reactions raise the temperatures of the reactor and thus provide a conducive environment for steam decomposition reaction 4 and carbon reduction reaction 6 increasing the amount of CO as shown in Figure 3. Increasing the air flow rate further provides more oxygen and most of the carbon is converted to CO_2 and some of the CO gets oxidized to CO_2. Methane concentrations are seen to decrease with increase of air flow rate. This is because increasing the air flow rate provides more oxygen and methane gas gets oxidized to carbon dioxide and water.

Effect of Air Flow Rate on Emissions

Any combustion process is rated clean or unclean depending on the levels of emissions. From the curve in Figure 4, it can be seen that the NO_x levels increased with increase of air flow rate. The SO_2 levels also increased slightly with increase in the air flow rate. NO_x is formed from reaction of nitrogen in air and oxygen and this reaction is dependent on prevailing temperatures as it requires high temperatures. Increasing the air flow rate led to increase in reactor temperature and that explains the increase in NO_x levels. SO_2 emissions on the other hand depend on the amount

ISSN: 2456-1851

Volume: 04, Issue: 05 "September-October 2019"

of sulfur in the fuel and since the amount of sulfur in the fuel is significantly small in this case 3.61%, the increase in SO_2 levels with increasing air flow rate is also small as shown in Figure 4.

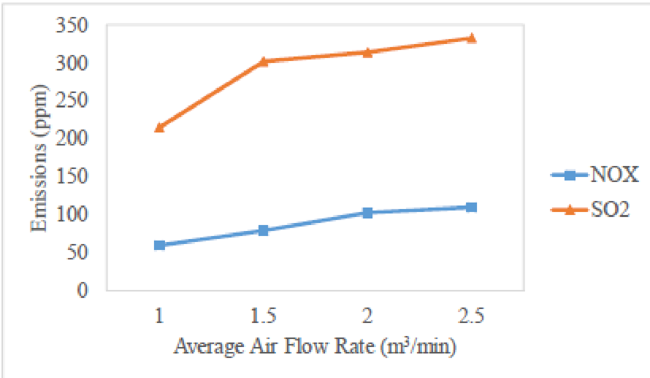

Figure 4: Emissions at various air flow Rates

The threshold limit value (TLV) for NO_x is 200 mg/m^3 (106 ppm) while that of SO_2 is 400 mg/m^3 (153 ppm) for old plants and 200 mg/m^3 (106 ppm) for new plants in European Union, China and Japan [22]. From the curve it can be seen that the NO_x exceeded its TLV value at airflow rate beyond 1.5 m^3/min while the SO_2 levels exceeded the TLV value for new plants.

Both NO_x and SO_2 are acidic gases and they react with water droplets in the atmosphere forming acid rain which can harm ecosystems. Inhaling large concentrations of this gases can irritate airways in human respiratory system and aggravate diseases like asthma. NO_x reacts with compounds in the atmosphere forming nitrite particles that form smog which reduces visibility. SO_2 on the other hand reacts with compounds in the atmosphere to form sulphate particles that form part of particulate matter which impairs visibility.

Effect of Air Flow Rate on Heating Value of Syngas

The HHV of the output syngas was noted to decrease with increase in air flow rate. From Figure 5, the HHV is relatively high for the first two flow rates. The calorific value of the syngas is dependent on the concentration of the combustible gases (CO, H_2 and CH_4). Increasing the air flow rate was noted to increase the concentrations of CO between air flow rates 1-1.5m^3/min and this explains the relatively high HHV. Increased concentration of N_2 which is non-combustible in the syngas as the air flow rate was increased further explains the decrease in the HHV of the syngas. The optimal air flow rate for which a maximum HHV of the syngas is obtained was deduced as 1.0 m^3/min to 1.5 m^3/min which corresponds to equivalence ratios 0.282 and 0.284.

ISSN: 2456-1851

Volume: 04, Issue: 05 "September-October 2019"

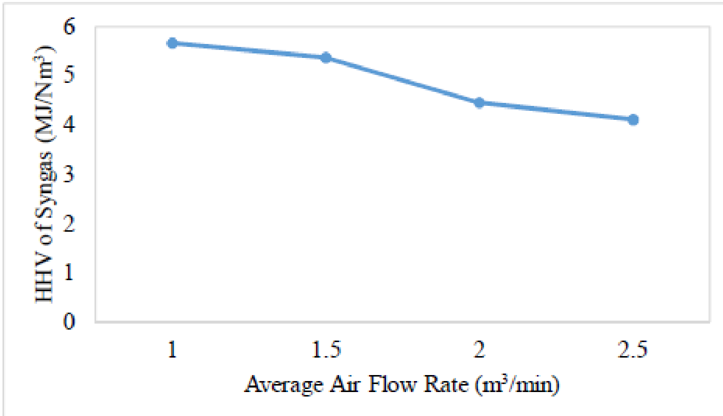

Figure 5: Syngas HHV variations with air flow Rate

Effect of Air flow Rate on the Reactor Temperature

The reactor temperature was seen to increase with increasing air flow rate as seen in Figure 6. Increasing the air flow rate increases the amount of oxygen available for combustion reactions 1, 2 and 3 which are exothermic and thus the temperature increase.

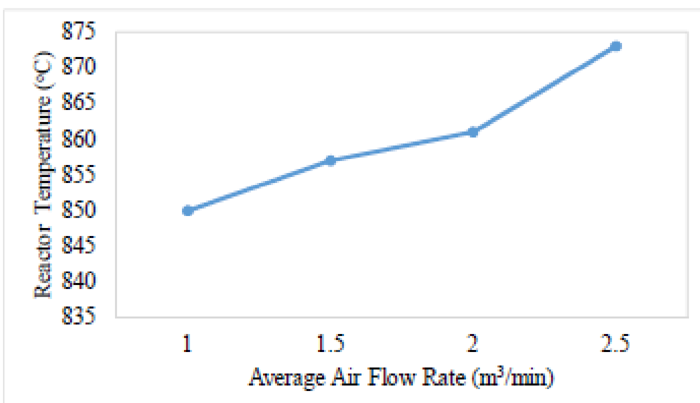

Figure 6: Reactor temperature variations with air flow rate

Cold Gas Efficiency and Carbon Conversion Efficiency

The cold gas efficiency of the gasifier corresponding to the optimal ER was obtained as 64.29%. The low CGE was because of high nitrogen concentrations in the syngas that lowered its heating value. The carbon conversion efficiency at the optimal ER was obtained as 89.89%. An average carbon conversion efficiency of 87.73% was obtained.

ISSN: 2456-1851

Volume: 04, Issue: 05 "September-October 2019"

4. CONCLUSION

Syngas composition was noted to vary with increase of air flow rate and the optimal equivalence ratio was established as 0.283. The HHV of the syngas at the optimal conditions was obtained as 5.667MJ/Nm^{3}which shows that the syngas produced can be used as fuel in for example gas turbines. The temperature inside the reactor was observed to increase with increase in air flow rate with the temperature at optimal ER being 857^{o}C.

Nomenclature

ϕ Sphericity

ϕ_s Sphericity of a sphere

ρ_f Density of fluidizing gas

ρ_s Density of coal particles

μ Viscosity of fluidizing gas

ε Void fraction

u Fluidization velocity

u_{mf} Minimum Fluidization velocity

u_t Terminal velocity

ΔP Pressure drop

h Bed height

g Acceleration due to gravity

REFERENCES

[1] P. E. Doerell, “All future energy will have to be ‘clean,’” *Appl. Energy*, vol. 64, no. 1–4, pp. 79–88, 1999.

[2] W. M, M. T, J. Gale, K. T. Eds, C. Henderson, and J. M. Topper, “CLEAN COAL TECHNOLOGIES AND THE PATH TO ZERO EMISSIONS,” *Greenh. Gas Control Technol.*, vol. II, pp. 1585–1591, 2005.

[3] R. W. Breault, “Gasification processes old and new: A basic review of the major technologies,” *Energies*, vol. 3, no. 2, pp. 216–240, 2010.

[4] Mamoru Kaiho and Osamu Yamadablished (National Institute of Advanced Industrial Science and Technology Japan), “Stoichiometric Approach to the Analysis of Coal

Gasification Process," in *Stoichiometry and Materials Science - When Numbers Matter*, D. A. Innocenti, Ed. intech: InTech, pp. 415–436.

[5] W. Nowak, "Clean coal fluidized-bed technology in Poland," *Appl. Energy 74*, vol. 74, pp. 405–413, 2003.

[6] N. Couto, A. Rouboa, V. Silva, E. Monteiro, and K. Bouziane, "Influence of the biomass gasification processes on the final composition of syngas," *Energy Procedia*, vol. 36, pp. 596–606, 2013.

[7] B. S. Dayananda and L. K. Sreepathi, "Design and Analysis of Fluidized Bed gasifier for Chicken Litter along with Agro Wastes," *Int. Res. J. Environ. Sci.*, vol. 1, no. 3, pp. 11–16, 2012.

[8] Professor Prabir Basu, *Combustion and Gasification In Fluidized Beds*. Taylor & Francis Group, LLC, 2006.

[9] A. A. M. Al-farraji, "Chemical Engineering and Reactor Design of a Fluidised Bed Gasifier," 2017.

[10] P. J. Van Den Enden and E. Silva, "Design approach for a biomass fed fluidized bed gasifier using the simulation software CSFB," *Biomass Bioenergy*, vol. 26, pp. 281–287, 2004.

[11] S. L. P. J.J. Ramirez, J.D. Martinez, "Basic Design of a Fluidized Bed gasifier for Rice Husk on a Pilot Scale," *Lat. Am. Appl. Res.*, vol. 37, pp. 299–306, 2007.

[12] D. K. Octave Levenspiel, *Fluidization Engineering*, 2nd ed. 1991.

[13] M. Hartman, O. Trnka, and K. Svoboda, "Fluidization characteristics of dolomite and calcined dolomite particles," *Chem. Eng. Sci.*, vol. 55, pp. 6269–6274, 2000.

[14] R. H. P. H. N. Don W. Green, *Perry's Chemical Engineer's Handbook*, 8th ed. 2007.

[15] A. E. Ghaly and K. N. Macdonald, "Mixing Patterns and Residence Time Determination in Bubbling Fluidized Bed System," *Am. J. Eng. Appl. Sci.*, vol. 5, no. 2, pp. 170–183, 2014.

ISSN: 2456-1851

Volume: 04, Issue: 05 "September-October 2019"

[16] K. G. S. Z. B. Jiu Huang, "Removal and Conversion of Tar in Syngas from Woody Biomass Gasification for Power Utilization Using Catalytic Hydrocracking," *Energies*, vol. 4, pp. 1163–1177, 2011.

[17] H. T. Wormsbecker Michael, Todd s. Pugsley, "The Influence of Distributor Design on Fluidized Bed Dryer Hydrodynamics Michael," 2007.

[18] A. Ergudenler and A. E. Ghaly, "Agglomeration of Alumina Sand in a Fluidized Bed Straw Gasifier at Elevated Temperatures," *Bioresour. Technol.*, vol. 43, pp. 259–268, 1993.

[19] A. E. Ghaly, A. Ergudenler, and V. V Ramakrishnan, "Effect of Distributor Plate Configuration on Pressure Drop in a Bubbling Fluidized Bed Reactor," *Adv. Res.*, vol. 3, no. 3, pp. 251–268, 2015.

[20] A. M. Shakorfow, "Operating and Performance Gasification Process Parameters," *Int. J. Sci. Res.*, vol. 5, no. 6, pp. 1768–1775, 2016.

[21] P. J. Ashman, A. Kosminski, S. J. Button, and P. J. Mullinger, "Gasification of Victorian Lignite in a Laboratory Scale Fluidised Bed Gasifier .," *5th Asia-Pacific Conf. Combust.*, no. July, pp. 18–20, 2005.

[22] X. Zhang, "Emission standards and control of PM 2 . 5 from coal-fired power plant," 2016.

[23] D. Tasma and K. Uzunanu, "'The effect of excess air ratio on syngas produced by gasification of agricultural residues briquettes,'" *Carbon N. Y.*, vol. 29, no. 24.85, pp. 22–60, 2007.

